Journal of Materials Chemistry A

Selective Electroreduction of CO2 to Carbon-rich Products by Simple Binary Copper Selenide Electrocatalyst

Journal:	*Journal of Materials Chemistry A*
Manuscript ID	TA-ART-11-2020-011518.R1
Article Type:	Paper
Date Submitted by the Author:	23-Jan-2021
Complete List of Authors:	Saxena, Apurv; Missouri University of Science & Technology, Chemistry Liyanage, Wipula; Missouri University of Science and Technology, Chemistry Masud, Jahangir; Missouri University of Science and Technology, Chemistry Kapila, Shubender; Missouri University of Science & Technology, Chemistry Nath, Manashi; Missouri University of Science & Technology, Chemistry

ARTICLE

Selective Electroreduction of CO_2 to Carbon-rich Products by Simple Binary Copper Selenide Electrocatalyst

Received 00th January 20xx,
Accepted 00th January 20xx

DOI: 10.1039/x0xx00000x

Apurv Saxena[a], Wipula Liyanage[a], Jahangir Masud[b], Shuben Kapila[a], Manashi Nath[a]*

In this article solvothermally synthesized copper selenide nanostructures have been resported as highly efficient electrocatalysts for carbon dioxide reduction under ambient conditions with high selectivity for carbon-rich C2 products at low applied potential. On addition to electrochemical measurements, density functional theory calculations were also performed to investigate adsorption energy of the key intermediate carbon monoxide on the catalyst surface. The authors proposed that CO adsorption energy on the surface can be a critical component to determine extent of CO_2 reduction on the surface, whereby a low CO adsorption energy was expecetd to yiled primarily C1 products while very large adsorption energy leads to catalyst posioning. In this article the authors have shown that by carefully designing catalyst surface to optimize CO adosrption energy and dwell time, selenide based electrocatalysts can indeed show more efficient CO_2 reduction compared to the base metal, leading to carbon-rich products. This is one of the first reports where Cu_2Se surface has been studied in details with experimental as well as DFT studies for CO_2 reduction. Interestingly, the reduction products showed dependence on applied potential forming exclusively formic acid at high applied potential (1.2 V and higher vs RHE) while ethanol and acetic acid were produced in high yield at potentials lower than 0.8 V vs RHE. The applied potential required for CO_2 with copper selenide was as low as 100 mV vs RHE, and is one of the lowest reported till date. The CO_2 reduction products were analyzed through NMR and GC TCD spectroscopy which showed ethanol and acetic acid production in excess of 80% Faradaic efficiency at low applied potential.

Introduction

While fossil fuel combustion continues to supply power to meet majority of global energy needs, the *Achilles heel* of the entire process is the production of copious quantities of carbon dioxide, CO_2 as a natural by-product. CO_2 representing the highest oxidation state of carbon, is a linear molecule containing sp-hybridized carbon doubly bonded to two O atoms. CO_2 is thermodynamically stable product and hence keeps enriching the atmosphere with increasing concentration. The natural escape route for atmospheric CO_2 is provided through sequestration by forest cover on the earth's surface, which over the past several decades has been depleted significantly making way for industrial landscape. While the effect of atmospheric CO_2 on global warming is a controversial topic in the current socio-political scenario, undisputed fact is that atmospheric carbon dioxide concentration is at an all-time high and is projected to rise in the next several years with a steeper slope.[1,2] Intergovernmental Panel on Climate Change (IPCC) in its 2018 report has indicated a strong risk of crisis as early as 2040 due to rising CO_2 levels in the atmosphere, which includes worsening food shortages and wildfires, and a mass die-off of coral reefs.[3-7] Currently CO_2 level in the atmosphere exceeds 400 ppm,[2] and CO_2 sequestration and storage will simply not be enough to combat this problem.[8] Hence a clever solution is direly needed whereby this huge amount of atmospheric CO_2 can be converted back to valuable chemical products thereby, closing the loop. However, CO_2 reduction reaction, (CO2RR) is a kinetically slow, energy intensive uphill reaction which necessitates the use of suitable catalysts that can lower the activation barrier and bring CO_2 out of the potential well. CO_2 is an extremely stable molecule with a high bond strength (~532 kJ/mol) and needs a high electrical potential to be activated in an electrochemical environment. Hence electrocatalysts which lowers this activation barrier, plays a predominant role for CO2RR and are considered to be the backbone of the entire process.[9-12] Although tremendous amount of research has been done for catalytic CO2RR,[13-22] catalyst design still presents a significant challenge in terms of product selectivity, lowering constraints of operating conditions (such as high voltage, pressure and temperature), and lastly economic feasibility.

Over the last several decades, significant amount of research has been conducted on converting CO_2 to other carbonaceous products through homogeneous[13-16] as well as heterogeneous catalysis.[17-22] Among the various catalysts reported for CO2RR, a major chunk includes precious metal based catalysts, such as Pt, Pd,[23] Ru, Au,[24] Ag[25] and their alloys. Recently, intensive research has led to identification of several non-precious

[a] Department of Chemistry, Missouri University of Science & Technology, Rolla, MO 65409, USA.
[b] Energy and Environmental Research centre, University of North Dakota, Grand Forks, USA
* *Email: nathm@mst.edu*
† Footnotes relating to the title and/or authors should appear here.
Electronic Supplementary Information (ESI) available: GC-TCD spectra, product quantification details from NMR spectra, calculation of Faradaic efficiency, structural models for DFT calculations, and band structure analysis. See DOI: 10.1039/x0xx00000x

transition metal based CO2RR catalysts based on Cu and Ni.[26-29] While this is definitely exciting from a practical point of view, the hindrance lies in range and selectivity of reduction products obtained. Typically, range of CO2RR products are categorized as *C1* or *C2* products depending on the formation and extent of C-C linkage. In most cases CO2RR with Cu- and Ni-based catalysts leads to a mixture of predominantly C1 reduction products primarily composed of carbon monoxide (CO), formate ion and formic acid, with trace amounts of formaldehyde or methanol.[28-30] While the lack of selectivity is a serious issue, the more detrimental fact is that CO, a toxic gas, is not a desirable product to be released in the atmosphere and hence must be reduced/processed further (typically through *syn gas* conversion) making the whole process tedious, cumbersome and less efficient. Rather, direct electroreduction of CO_2 to alcohols or other value-added hydrocarbons with higher carbon content (C2 or higher) is more desirable.

Among the various transition metals studied for CO2RR, Cu has attracted most attention due to the range of reduction products formed under ambient conditions as well as feasible electroreduction of CO_2 at low applied potential.[31] Bulk Cu as well as Cu nanoparticles has been shown to primarily produce CO and CH_4. Hori *et al.*[32] reported extensive study of CO_2 electroreduction using Cu electrodes and described the product distribution at different applied potentials. C_1-C_3 products were produced when the CO2RR was carried out in presence of Cu.[31] It has been claimed that size of Cu nanoparticles also has an effect on CO_2 reduction products.[33] Even morphology and surface roughness of Cu can effect Faradaic efficiency and selectivity of the reduction products. [34] Cu films oxidized on the surface gives some C2 products.[35] Cu nanocrystals produces formic acid (HCO_2H) at -0.5V (vs RHE) with Faradaic efficiency of 28%.[36] Cu fibers and Cu nanowires also showed selectivity at different applied potential. Variation of crystal dimensions also led to selectivity for different products. Fe porphyrin on CNTs showed CO2RR activity producing CO at 0.5 V overpotential.[37] It was observed that doping can also influence the electrocatalytic properties with respect to CO2RR. For example, products of CO_2 reduction with boron doped diamond vary in amount as a function of boron content and maximum Faradaic efficiency (75%) for producing formic acid was obtained with boron content of 0.1%. The Faradaic efficiency decreased with increasing boron content.[38] Multiphase systems like Cu on TiO_2, Ag on TiO_2 or $In(OH)_3$ were also observed to be photocatalytically active for CO2RR with a 97% conversion to CH_4 under normal solar illumination.[39] Cu_2O has also been reported as a electrocatalyst for CO2RR.[40] In addition, WSe_2 and $MoSe_2$ has also shown good activity for CO2RR.[41] Although Cu has proved to be a cheap and energy efficient electrocatalyst for the CO_2 reduction, the lack of product selectivity at room temperature under ambient conditions has been less than ideal, leaving plenty of room for improvement in catalyst performances.[42] Although Faradaic efficiency of CO2RR products formed from metal-based electrocatalysts (Cu, Ni, Au, Ag, and Pd) are reasonable, they suffer from several major drawbacks, the most concerning being poisoning of the catalyst surface with CO and other reaction intermediates, and deactivation of the catalysts within a small time. These metallic electrocatalysts also have very low Faradaic efficiency for C2 or higher carbon-rich products.[43-45] Surface modification of the metal catalysts by forming oxide layers could reduce the catalyst poisoning and deactivation problems slightly. However, with Cu_2O electrode, the Faradaic efficiency of the hydrocarbon products were also reduced compared to Cu, and CO became one of the major products again. Hence, while Cu_2O showed sustained catalytic activity for CO_2 reduction compared to Cu, lower Faradaic efficiency and lesser product selectivity, leads to the feasibility of Cu_2O as practical CO2RR electrocatalyst as being severely challenging.[46] In a study by Ramirez and coworkers, experimental and theoretical study of chalcogen modified copper for CO2 electroreduction was performed which resulted in selective electroreduction of CO_2 into formate. This study concluded that formate generation happens because of presence of basic sites where CO_2 was secured preventing its dissociation toward CO.[47,48]

Previously it has been reported that reducing anion electronegativity around the catalytically active transition metal site leads to better modulation of electrochemical redox of the catalytic site leading to lowering of the activation energy for electrocatalytic activity. Hence, we propose that Cu-based chalcogenides will show better electrocatalytic activity for CO2RR at lower applied potential compared to oxides and the base metal. Moreover, we further propose that reducing anion electronegativity will also lead to enrichment of electron density around the transition metal center, which will influence binding energy of CO intermediate on the surface, which becomes crucial for preferential formation of C1 and C2 reduction products. Specifically, we have proposed that optimal CO adsorption energy on the catalyst site is required to maximize dwell time of CO intermediate on the surface, enough for further reduction to form carbon-rich products, while weak CO adsorption energy leads to ready desorption of C1 products (CO and formic acid). High CO adsorption energy, on the other hand, leads to catalyst surface poisoning. We have applied this concept to design selenide based electrocatalyst surface as optimal catalyst for CO2RR producing carbon-rich products.

In this article we have reported the highly efficient electrocatalytic activity of copper selenide (Cu_2Se) nanostructures obtained via solvothermal method. Cu_2Se nanoparticles exhibited enhanced CO2RR activity at low applied potential ranging from -0.1 to -1.3 V vs RHE with high product selectivity, high Faradaic efficiency, and functional stability for prolonged period of time. At very low negative potentials, C2 products like ethanol and acetic acid were obtained selectively, whereas at high negative potentials, C1 product such as formic acid was obtained almost exclusively. Interestingly, no CO was detected in the product composition. We have also performed density functional theory (DFT) calculations to estimate CO binding energy on the catalyst surface and correlate that with typical CO2RR products obtained with various catalyst systems (Cu_2Se, Cu_2O, Cu etc.) and validate our hypothesis regarding CO adsorption energy and preferential formation of C1/C2 products. Interestingly CO2RR with this electrocatalyst could be performed under ambient condition at room temperature with

a slow stream of CO_2 as feedstock. This will be ideal to reduce CO_2 at various sources including diffuse sources as well as points of generation such as coal or gas-fired power plants.

Experimental Methods

Material

Cuprous oxide (Cu_2O, 99%), selenium, hydrazine (99.5%) and $NaHCO_3$ (99.7%) were purchased from Sigma-Aldrich and used without purification. Deionized water was used to prepare all solutions and to rinse samples and glassware.

Solvothermal synthesis of Cu_2Se

1.0 mmol Cu_2O was mixed in 5.0 ml of H_2O and stirred for 15 minutes. Then 1.0 mmol Se powder was added to the reaction mixture and stirred for another 30 minutes. 2.0 ml of hydrazine ($N_2H_4.H_2O$) was added dropwise to the mixture with continuous stirring for 10 minutes. The resulting solution was transferred to a polytetrafluoroethylene (PTFE) lined stainless-steel autoclave. The autoclave was sealed and maintained at 185 °C for 24 h, then cooled naturally to room temperature. The product formed was washed and centrifuged for several times with DI water and then with mixture of ethanol and water to remove impurities and unreacted precursors. Lastly, the product was dried in a vacuum oven at 35°C for 24 h.

Preparation of electrodes

To check the activity of copper selenide powder, the working electrodes were prepared by drop-casting catalyst ink on carbon fiber paper (CFP). Typically, a catalyst ink was prepared by dispersing 5 mg of catalyst (copper selenide) powder in 250 µL Nafion solution (50 µL of 1% Nafion solution in 50 µL of 50% IPA in water). After 30 minutes of ultrasonication, 50 µL of the dispersion was drop casted on a confined area (2 cm^2) on carbon fiber paper substrate. The drop-casted Cu_2Se@CFP film was then dried at room temperature and further heated at 130 °C for 30 minutes in an oven.

Preparation of electrolyte

$NaHCO_3$ aqueous solution was used as electrolyte for CO2RR. 0.3M $NaHCO_3$ electrolyte solution was prepared from stock solutions of higher concentration in DI water, which were then diluted to the target molarity.

Methods of characterization

Powder X-ray diffraction: The crystalline phase of as-synthesized catalyst powder was identified through powder X-ray diffraction (pxrd) with Philips X-Pert utilizing CuKα (1.5418Å) radiation. Pxrd pattern was collected from the pristine product with no further treatments.

Scanning electron microscopy (SEM): SEM images of the Cu_2Se-modified electrode surfaces was obtained using a FEI Helios NanoLab 600 FIB/FESEM at an acceleration voltage of 10 kV and a working distance of 4.8 mm. Energy dispersive spectroscopy (EDS) along with line scan analysis was also obtained from the SEM microscope.

X-ray photoelectron spectroscopy (XPS): The oxidation states of the elements in copper selenide samples were investigated by X-ray photoelectron spectroscopy (XPS) using the KRATOS AXIS X-ray Photoelectron Spectrometer with monochromatic Al

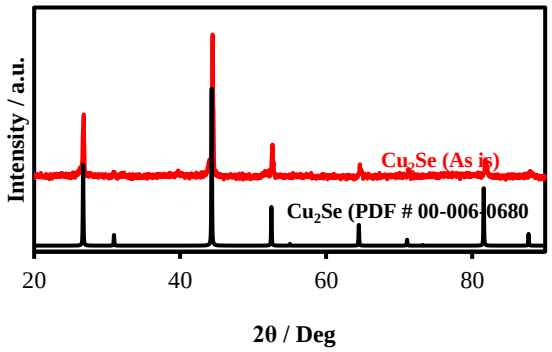

Fig. 1. PXRD pattern of hydrothermally synthesized Cu_2Se compared with the standard Cu_2Se reference pattern (PDF # 00-006-0680).

X-ray source. All XPS measurements of the catalyst surface were collected as-is without sputtering. C1s signal at 284.5 eV was used as a reference to calibrate all the XPS binding energies.

Electrochemical characterization and electrocatalytic studies: Electrochemical H-cell was used in this study consisting of separate cathode and anode compartments with a volume of 30 ml each, separated by an anion exchange Nafion (115) membrane. The linear sweep voltammetry (LSV) was performed in N_2-saturated and CO_2 saturated 0.3 M $NaHCO_3$ electrolyte with a scan rate of 10 $mV.s^{-1}$. In this study carbon rod was used as counter electrode, Cu_2Se@CFP and $Ag|AgCl|KCl_{(sat.)}$ were used as working and reference electrodes, respectively. The $Ag|AgCl$ reference electrode was calibrated using open circuit potential (OCP, −0.199 V) measured with a Pt wire in H_2-saturated H_2SO_4 solution. The potential measured in $Ag|AgCl$ was converted to reversible hydrogen electrode (RHE) using the eq. 1:

$$E_{RHE} = E_{Ag|AgCl} + 0.059pH + E^0_{Ag|AgCl} \quad ---(1)$$

where E_{RHE} is the converted potential vs RHE, $E_{Ag|AgCl}$ is the experimentally obtained potential, $E^\circ_{Ag|AgCl}$ is the standard potential of $Ag|AgCl$ (0.199 V), and the pH of CO_2 saturated 0.3 M $NaHCO_3$ was measured to be 6.8. 0.3M $NaHCO_3$ in cathode compartment was saturated with CO_2 through continuous purging at the rate of 10 sccm using mass controller during the experiments.

Tafel plots: For explaining the kinetics of a reaction and electrocatalytic activity, Tafel slope is an important parameter. and Tafel equation can be expressed as follows:

$$\eta = \alpha + (2.3R\,T)\log j/\alpha nF \quad --- (2)$$

where η is the overpotential, α is the transfer coefficient, n is the number of electrons involved in the reaction, F is the Faraday constant, j is the current density and the slope is given by 2.3RT/ αnF.

The Tafel equation as shown in eqn. (2) is a fundamental equation which acquires from the kinetically controlled region of CO2RR and relates the overpotential Z with current density j

where the Tafel slope is given by 2.3RT/anF. To calculate Tafel slopes, LSV plots were obtained with a slow scan speed (10 mV s^{-1}) in non-stirred solution.

RESULTS AND DISCUSSION

Structure and morphology of Cu_2Se

Composition and phase of the hydrothermally synthesized product was ascertained with XPS and pxrd, respectively. The pxrd pattern as shown in Figure 1 confirmed that the as-synthesized product was primarily composed of crystalline Cu_2Se and the diffraction lines could be well-matched with that of standard Cu_2Se phase (PDF# 00-006-0680).

Morphology of the product was studied through SEM which showed that the hydrothermally synthesized Cu_2Se formed nanocubes (Figures 2a and b) with sizes in the range of 100 nm – 1 µm and exhibiting considerable surface roughness. These granular nanocubes were comprised of Cu and Se with a relative atomic ratio of approximately 2:1, respectively, as shown in Figure 2c. The EDS measurements were typically performed on different regions of catalyst surface to confirm uniformity of composition. While EDS confirmed the presence of Cu and Se uniformly throughout the sample, it also confirmed absence of even trace amounts of oxygen, confirming that the sample composition was indeed pure Cu_2Se.

The composition of the catalyst was also confirmed through XPS studies. Figure 2d represents the deconvoluted Cu 2p XPS peak for as-synthesized Cu_2Se catalyst where the peaks at 932.8 and 953.1 eV for Cu^{1+} $2p_{3/2}$ and $2p_{1/2}$ peaks and 934.1 and 954.8 eV for Cu^{2+} $2p_{3/2}$ and $2p_{1/2}$ peaks, confirmed the presence of Cu in +1/+2 mixed oxidation states.[49] The coexistence of +1 and +2 mixed valence states for Cu has been reported previously in Cu_2Se.[40] The deconvoluted Se 3d XPS spectra (Figure 2e) showed peaks at 54.5 and 55.3 eV corresponding to Se $3d_{5/2}$ and Se $3d_{3/2}$, respectively, in accordance with previously reported spectra for Cu_2Se.[49] The oxidation state of Se was estimated to be Se^{2-} by comparison with previously reported literature.[49] The relative ratio of Cu^{2+} and Cu^{+} was also estimated from the deconvoluted XPS spectra as shown in Fig. 2 using area under the peaks. A Cu^{2+}:Cu^{+} ratio of 1.07 was obtained for the pristine catalyst. These XPS results along with pxrd confirmed that the predominant phase of these solvothermally synthesized catalyst powder was Cu_2Se. Comparison of XPS spectra collected before and after long-term electrolysis shows that Cu and Se XPS peaks do not change positions indicating no change in oxidation states and/or coordination geometry. The Cu+:Cu2+ ratio after prolonged CO2RR activity shows minimal change (Cu2+:Cu+=1.07) compared to pristine sample. Selenium oxidation state remains -2, same as before activity.

Electrochemical performance and CO2RR catalytic activities

The solvothermally synthesized Cu_2Se powder was assembled onto a CFP electrode following method as described in the methods section. A typical catalyst loading of 1.25 mg.cm^{-2} was used for most electrochemical measurements reported in this manuscript. To investigate the electrocatalytic property of Cu_2Se towards CO_2 reduction, electrochemical studies were performed in 0.3 M $NaHCO_3$ solution (pH = 6.8) with continuous purging of CO_2 gas at room temperature under ambient pressure. The electrochemically active surface area (ECSA) of the catalyst composite was calculated from electrochemical double layer capacitance as a function of scan rate measured in

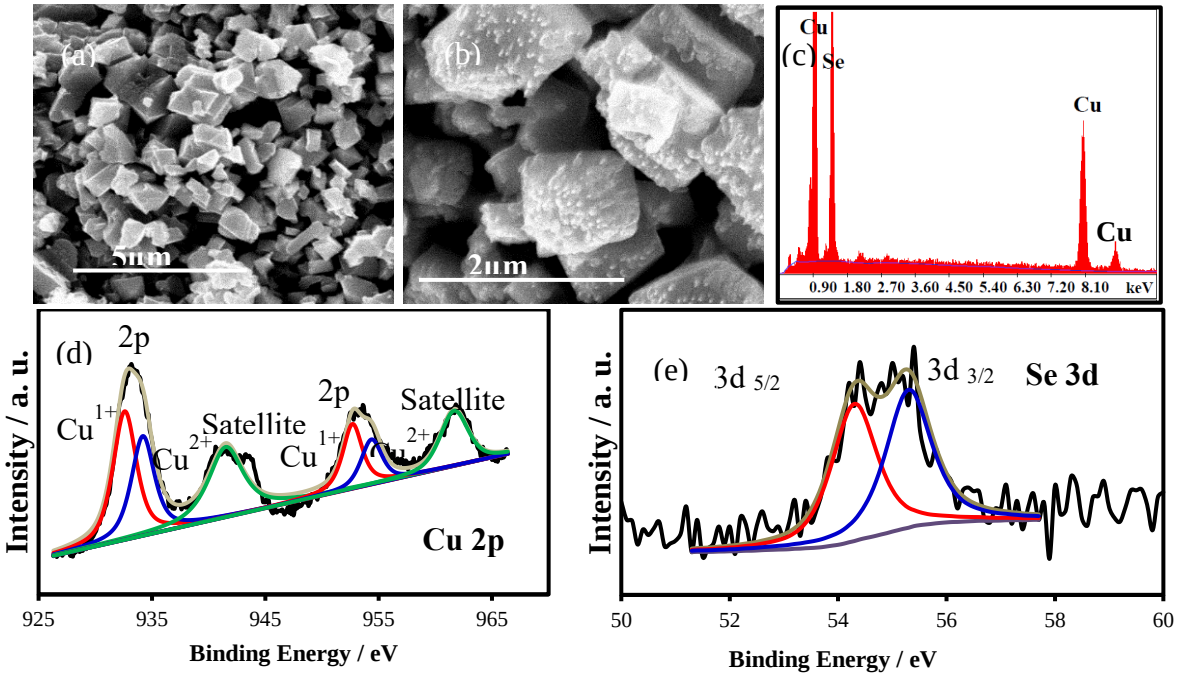

Fig. 2 SEM images of the Cu2Se nanoparticles at (a) low and (b) high magnification showing formation of nanocubes and surface roughness, respectively. (c) EDS analysis of the catalyst confirming presence of Cu and Se in 2:1 relative atomic ratio. (d) Cu 2p and (e) Se 3d XPS spectra of as-synthesized Cu_2Se.

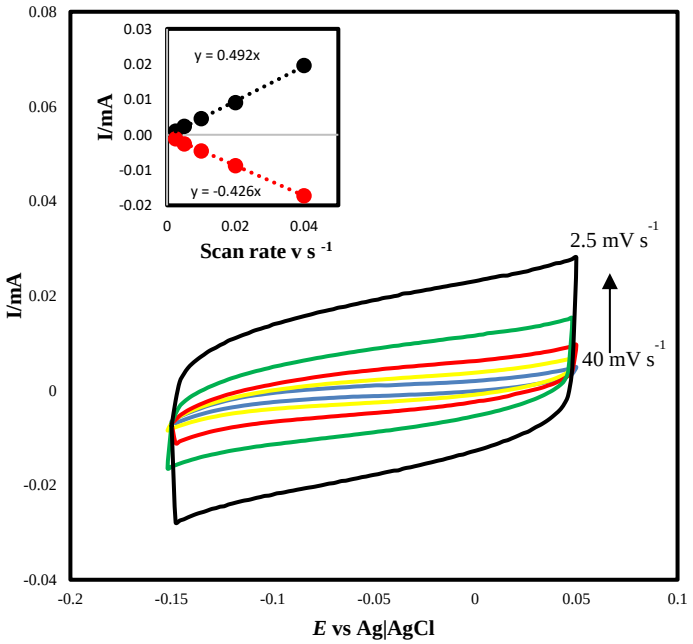

Fig 3. Cyclic voltammograms measured for Cu_2Se catalyst in 0.3 M $NaHCO_3$ at continuous N_2 purging at different scan rates from 2.5 to 40 mV s^{-1}. Inset shows plot of anodic and cathodic current measured at 0.044 V vs Ag|Agcl as function of scan rate.

the non-Faradaic region (Figure 3), and comparing this capacitance with the specific capacitance (C_S) obtained from the literature.[49] The double layer capacitance (C_{DL}) was estimated by using equation (3) wherein, i_{DL} is the measured current and v is the scan rate.

$i_{DL} = C_{DL} \times v$ --- (3)

ECSA = CDL/Cs ---(4)

C_{DL} estimated from the *i* vs *v* plot as shown in inset of Fig. 3 gave a value of 0.49 mF. ECSA estimated as the ratio between C_{DL} and C_S (eqn. 4), was calculated to be 12.25 cm^2 using a C_S value of 40µF cm^{-2}, typical of the electrolyte as reported in previous literature.[49] The roughness factor (RF) of the electrode composite estimated from the ratio between ECSA and geometric area, was estimated to be 153.12. A high ECSA and roughness factor typically signifies a rough catalyst surface which facilitates electrolyte access to the catalytically active sites and hence is expected to enhance electrocatalytic activity. The CO2RR activity of Cu_2Se modified CFP electrode was checked by measuring the current-voltage polarization curves in 0.3M $NaHCO_3$ solution in presence and absence of dissolved CO_2 introduced in the solution by purging. Similar measurements were also performed with blank CFP electrode to study the effect of substrate only as shown in Figure 4a. It was observed that blank CFP did not show much current response in absence of CO_2. Purging the solution with CO_2 changed the polarization curve for the CFP very slightly. The Cu_2Se@CFP electrode on the other hand, showed a significant change in the polarization curve in presence of dissolved CO_2 in the bicarbonate-based electrolyte as can be seen in the Figure 4a. A significant reduction current was observed between 0.2 and −0.4 V vs RHE for Cu_2Se@CFP electrode in presence of CO_2 similar to those reported previously for other CO2RR systems such as Pd layers deposited on Pt (Pd−Pt)[9]. This reduction current can be due to either direct carbon dioxide reduction on the electrode surface or indirect reduction of bicarbonate anion (HCO_3^-) to formate/formic acid. It has been reported previously that as pH decreases near the electrode surface with decreasing potential due to continuous hydrogen evolution,[24] in situ conversion of CO_2 to HCO_3^- occurs. However, such spontaneous conversion occurs at high concentration of nascent hydrogen and consequently at higher applied potential. From the linear sweep voltammetry (LSV) studies as shown in Figure 4, it was confirmed that although CFP was minimally responsive towards CO2RR, the Cu_2Se-modified CFP has high catalytic activity towards CO2RR and can exhibit high current density in excess of 50 mA.cm^{-2} at low applied potential.

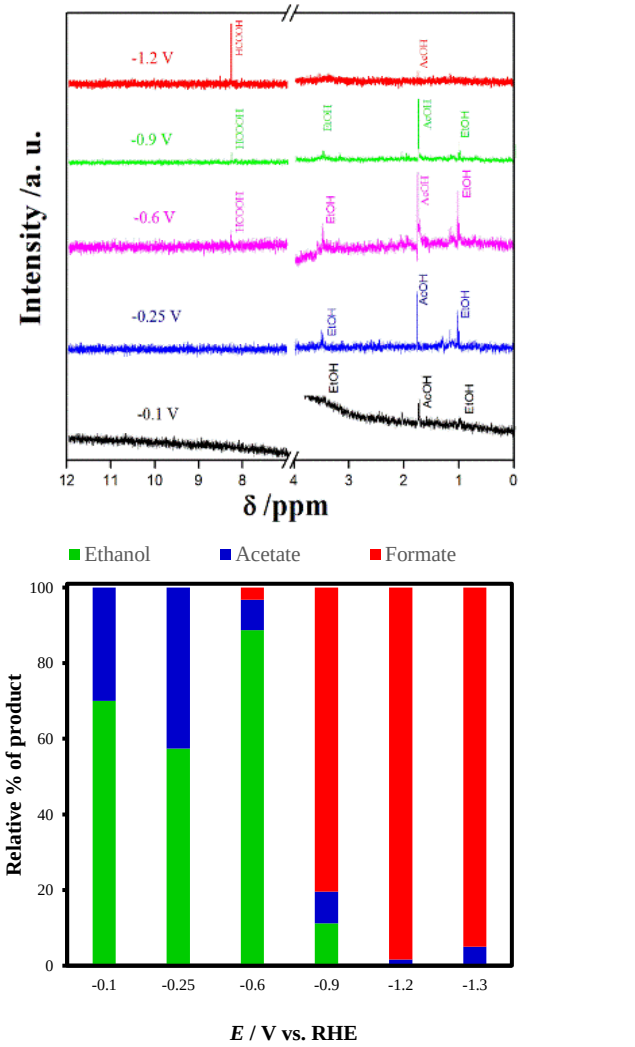

Fig.5 (a) NMR spectra identifying reduction products in reaction aliquots collected at different potentials. (b) Bar plot depicting relative concentrations of liquid products quantified from NMR at different stationary applied potentials.

Kinetics of CO_2 electrochemical reduction on Cu_2Se@CFP was also studied through Tafel plots as shown in Figure 4b. The Tafel slope was estimated to be 126.8mV dec^{-1} for the CO_2 electroreduction on Cu_2Se@CFP electrode which is much smaller than the Tafel slope of only CFP substrate indicating that electron transfer from the Cu2Se modified electrode surface is much faster. It should be also noted that the Tafel slope of CO_2RR (126.8mV dec^{-1}) on Cu_2Se is different than that of

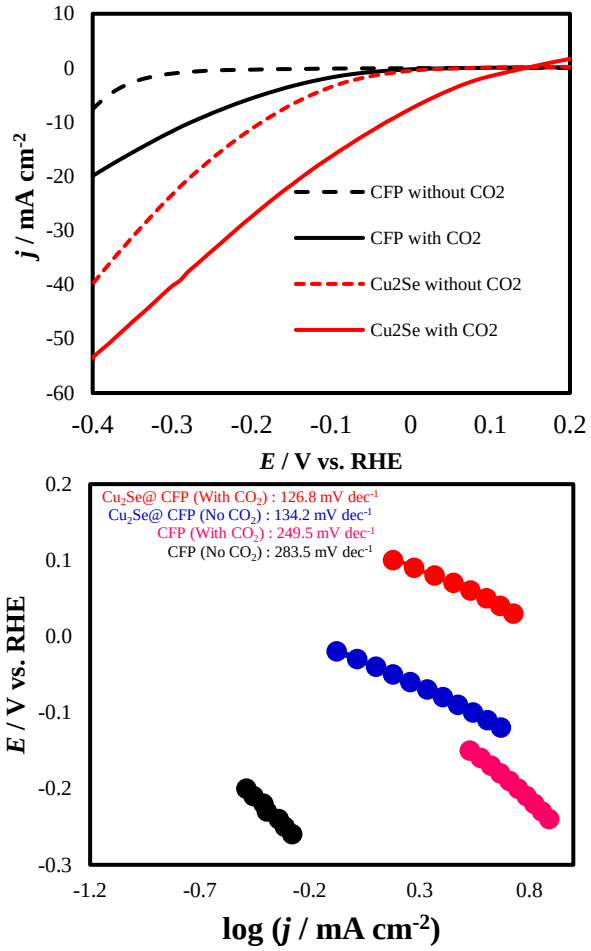

Fig 4. (a) LSVs measured in 0.3M $NaHCO_3$ at a scan rate of 10 mV s^{-1} in presence and absence of CO_2 with different electrodes. (b) Tafel plots measured in 0.3 M $NaHCO_3$.

protonation (134.2 mV dec^{-1}) which was calculated from polarization curve of Cu_2Se@CFP electrode without CO_2 purging. Tafel slopes typically provide insight regarding reaction kinetics as well as information about the rate determining step. The Tafel slope obtained for Cu_2Se catalyst was comparable to other CO2RR electrocatalyst systems.[50,51]

To analyze the composition of different products being formed through CO_2RR on Cu_2Se@CFP electrodes, CO_2 electroreduction were performed at different applied potentials (-1.3 V, -1.2 V, -0.9 V, -0.6 V, -0.25 V, -0.1 V vs RHE) held constant for 1 h in 0.3M $NaHCO_3$ under constant purging with CO_2 gas at low flow rate (20 sccm). The gaseous products from CO_2 reduction were examined with gas chromatography equipped with thermal conductivity detector (GC-TCD) (Fig. S1), while the liquid products were quantified by ^{1}H NMR spectroscopy (Table S1). It was observed that the CO_2RR products chemistry was dependent on the applied potential and exhibited a significant product selectivity as can be seen in the NMR plots (Figure 5a) collected at different applied potential. Interestingly, it was observed that at low applied potential the reduction products consisted of exclusively higher carbon-content compositions such as ethanol and acetic acid. As applied potential was increased, the amount of these carbon-rich products (ethanol, acetic acid) increased in yield, while above -0.6 V (vs RHE) minute quantities of C_1 product such as formic acid could be detected along with ethanol and acetic acid. As the applied potential was increased even further, amount of formic acid production increased along with decrease in the relative quantities of ethanol and acetic acid. At significantly higher applied potential (-1.2 V vs RHE) the product formed was exclusively formic acid as detected through NMR (Figure 5a). The relative product yields at different potentials was estimated by quantifying the NMR plots as mentioned in supporting information (Table S2). Figure 5b shows the product selectivity at different applied potential. It was observed that at lower applied potential C2 products formed more preferably while the C1 products formed exclusively at higher applied potential. Such product selectivity is extremely important for practical implementation of catalytic CO2RR as a viable technology. More importantly, formation of higher carbon-rich fuels such as ethanol with high selectivity at low applied potential and consequently with lesser energy expenditure, will also have significant implication in practical application of these CO2RR reactions. The gaseous products formed at different applied potential was also investigated by collecting the head space gas after 1 h of CO2RR. Interestingly no carbon monoxide (CO) was detected while there was minimal production of H_2 at high applied potential. Production of H_2 increased considerably at higher applied potential (-0.9 V vs RHE and above). HER is known to compete with CO2RR and it has been a challenge to design catalyst surfaces that will suppress HER while favoring CO2RR. For Cu_2Se-modified electrodes, since CO2RR can occur at much lower applied potential than required for HER, production of hydrogen is inhibited, while hydrocarbon production is enhanced at low potentials. The total Faradaic efficiency for CO2RR was calculated by considering both liquid and gas phase products quantified through GC-TCD and NMR analysis performed on the same experimental set-up and taking into account all the products that were detected. Typically, electron mole fraction required for each product formation was used along with the product mole fraction estimated from GC-TCD (gaseous products) or NMR spectra (liquid products) and total charge consumed for each period of time, to calculate Faradaic efficiency. The total product percentage at any specific potential was obtained by adding the product quantification data from GC-TCD and NMR experiments. Figure 6 shows the Faradaic efficiency and relative percentages of all reduction products detected (through combined GC-TCD and NMR analysis) at each applied potential. It was observed that while H_2 was generated at high negative potential, there was no

production of CO within detectable range of GC-TCD. Hydrocarbons such as methane, ethane etc. were also absent from the products possibly due to les availability of reactive hydrogen at such low applied potentials. As mentioned above Faradaic efficiency for CO_2 reduction was calculated by considering the total charge consumed and quantifying products detected in NMR and GC-TCD. An optimal condition was observed for C1 products at an applied potential of −1.2 V vs RHE wherein formic acid was produced with 98.33% product selectivity after 1 h of electrolysis with high Faradaic efficiency. For potentials higher than −1.2 V vs RHE, the maximum faradaic efficiency (for formic acid) decreased to 94 % (−1.3 V vs RHE), which also showed deactivation over time (Table S4). For lower

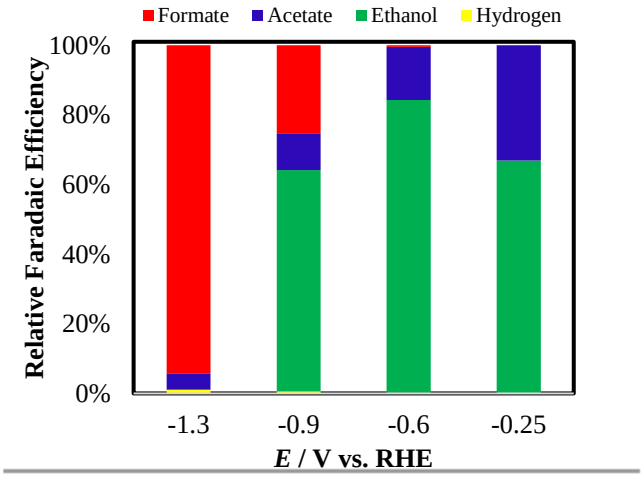

Fig 6. Bar plot depicting relative faradaic efficiency of liquid as well as gas products at different applied potentials.

applied potentials (−0.9, −0.6, and −0.25 V vs RHE) C1 products showed decrease in Faradaic efficiency (25.26 %, 0.5 %, and 0 %, for formic acid at -0.9, -0.6, and -0.25 V, respectively) while relative yield of C2 products increased. Details of estimation of the Faradaic efficiency for each reduction product at various applied potentials has been provided in supporting information (Tables S2, S3). At -0.6 V, Faradaic efficiency in excess of 84 % was observed for ethanol. It must be noted here that such high Faradaic efficiency for C2 product such as ethanol has been observed very rarely. Hence the novelty of this simple binary copper selenide based electrocatalyst lies in its ability to produce carbon rich fuels with high selectivity and Faradaic efficiency at low energy expense. Moreover, this Cu_2Se-based catalyst also exhibits high current density exceeding 50 $mA.cm^{-2}$ at moderately low applied potential.

The stability of Cu_2Se electrocatalyst for long-term CO2RR activity was also investigated by carrying out the electrochemical carbon dioxide reduction under constant applied potential for extended period of time, typically 12, 24 or 100 h. These are typically referred to as chronoamperometry measurement where potential is kept constant for extended period of time while current density is measured. Typical chronoamperometry plots measured at different applied potentials has been shown in Figures S2a (12 h at -0.1 V, -0.6 V, and -0.9 V vs RHE), S3 (24h at -0.9 V vs RHE) and S4 (100 h at -

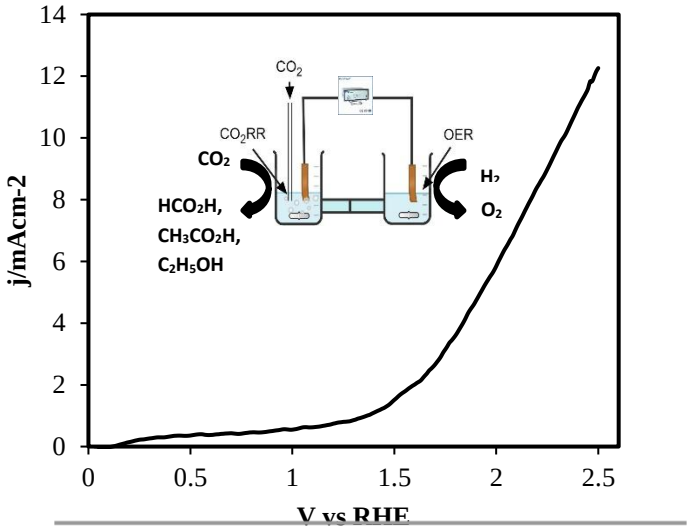

Fig. 7. Polarization curve with cathodic CO2RR and anodic OER with Cu_2Se@CFP as both cathodic and anodic electrocatalyst. Inset shows schematic of the electrochemical setup for combined CO2RR and OER.

0.6 V vs RHE). As can be seen from these plots, the reduction current density did not any change for extended period of time indicating the catalyst was functionally stable under conditions of continuous CO2RR under an applied potential. The product composition analyzed by NMR after chronoamperometry studies showed similar relative percentages as shown in Figure 5. The catalyst composition after long-term electrolysis under an applied potential was also investigated through pxrd and XPS analysis. Pxrd pattern of the catalyst film after 24 h of CO2RR at -0.9 V was superimposable with that of pristine Cu_2Se as shown in Figure S2b, indicating that there was no change in the crystalline phase of the catalyst. XPS analysis of the catalyst film after chronoamperometry studies has been shown in Figure S2c – f, which shows Cu2p and Se 3d peaks which are exactly superimposable with that of the pristine catalyst, with no change in peak positions indicating no change in oxidation states and/or coordination geometry. The Cu^{2+}:Cu^{+} ratio estimated from the deconvoluted XPS spectra was obtained as 1.07, similar to the pristine catalyst composition. Hence, pxrd and XPS analysis confirmed that the catalyst was also compositionally stable after extended period of catalytic activity.

It must be noted here that Cu_2Se has also been reported recently as an efficient electrocatalyst for oxygen evolution reaction (OER) in alkaline medium with an onset potential of 1.42 V (vs RHE) and overpotential of 310 mV at 10 $mA.cm^{-2}$.[49] Hence Cu_2Se can be ideally used as a bifunctional catalyst that can reduce atmospheric CO_2 while simultaneously enriching the air with oxygen produced through water electrolysis. The bifunctionality of this catalyst was probed by constructing an electrochemical H-cell containing alkaline electrolyte (1M KOH) in the anodic chamber and bicarbonate solution in the cathodic chamber. The two electrolyte chambers were separated by Nafion membrane and it was confirmed that there was no enrichment of OH^- in the cathodic chamber. CO_2 was purged in the cathodic chamber. Inset in Figure 7 shows schematic representation of the electrochemical cell along with the LSV

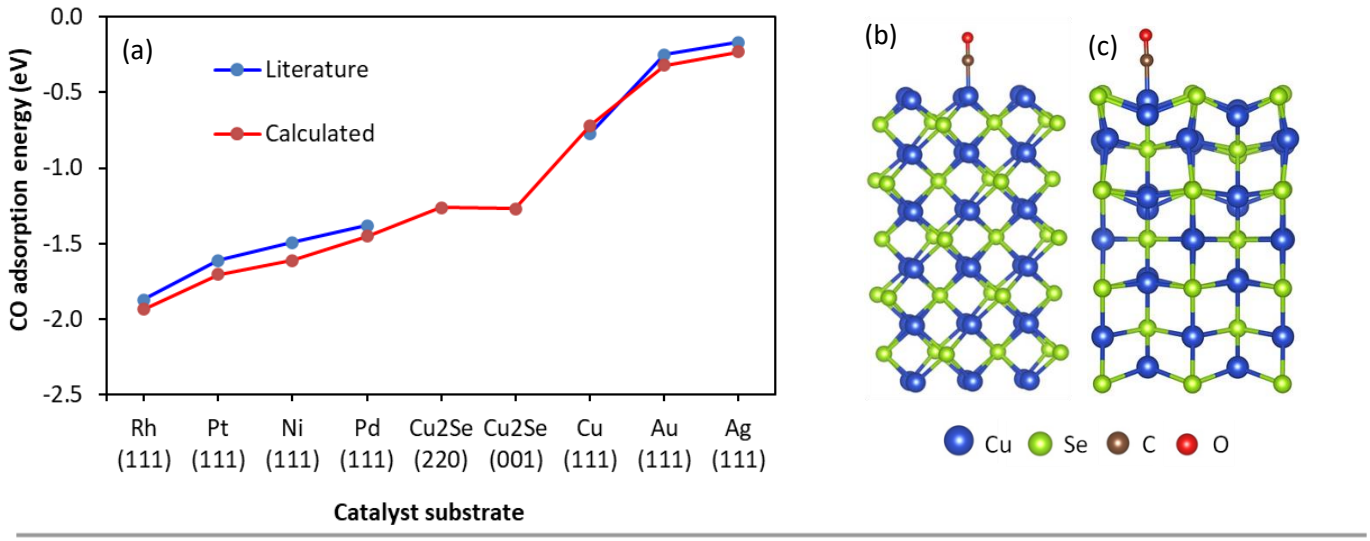

Fig. 8. Comparison of calculated CO adsorption energy on known catalyst materials with Cu_2Se. (a) CO adsorption on Cu_2Se was calculated on (001) surface and (220) surface while for the metals it was calculated on (111) surfaces. Reported values were selected from data that has used the same functional as the present study for calculation of adsorption energies.[52,53] Adsorption configurations used for calculation of (b) CO on (001) surface (c) CO on (220) surfaces.

plot obtained from the CO2RR-OER combined experiment. Potential was scanned in the anodic direction whereby O_2 evolution was observed in the anode concurrent with the rise in oxidation current. The reduction products in catholyte were analyzed by collecting the aliquot from cathode chamber after 12 hours of continuous CO_2RR-OER at 2 V. NMR analysis of the catholyte showed that they contained primarily formic acid, acetic acid, and ethanol analogous to product composition observed previously in Figure 5.

Exploring CO Adsorption Energies on Catalyst Surfaces

The excellent activity of Cu_2Se was also investigated using density functional theory (DFT) to further understand enhanced performance of the catalyst and selectivity towards carbon-enriched reduction products. Details of the DFT calculation has been provided in the supporting information. Previously it has been shown that amongst numerous pathways to electrochemically reduce CO_2 to various hydrocarbon products on the catalyst surface, one of the key intermediates is CO.[52] Reduction of CO_2 to CO is a two electron transfer process as schematically illustrated in Figure S5 in supporting information. First, a proton-electron pair (H^+/e^-) is transferred to the CO_2 adsorbed on the catalyst-electrode which is then reduced to a carboxyl intermediate *COOH (where * denotes adsorbed species on the catalyst surface). Then a second H^+/e^- pair participate in further reduction of *COOH to *CO and H_2O.[52] Although the conversion of *COOH to *CO takes place readily, the conversion of CO_2 to *COOH was found to be limited by the weak binding of COOH to the catalyst surface.[53] This elementary reaction step of CO_2 adsorption on Cu_2Se surface was simulated as shown in Figure S5(b), and it was observed that *COOH intermediate can form a stable configuration with the formation of Cu-C and Cu-O bonds with adjacent Cu atoms on the surface of Cu_2Se which is similar to stable *COOH configurations previously reported by other researchers.[53,54] Hence, favorable binding of *COOH on Cu_2Se accelerates the formation of *CO intermediate on catalyst surface.

A primary hypothesis is being proposed in this manuscript regarding catalyst design to promote preferential formation of carbon-rich (C2 and C3) reduction product. It can be expected that *CO dwell time on the catalyst surface is a key parameter for preferential formation of C1 or C2/C3 reduction products. The *CO dwell time can be directly related to the CO adsorption energy on the catalyst site. If *CO is weakly bound to the catalyst surface, it can desorb readily forming carbon monoxide (CO) as the major product.[52] Hence, a moderately higher *CO adsorption energy is essential for retaining *CO on the catalyst surface long enough for facilitating continuous reduction of *CO to higher hydrocarbons such as methanol and ethanol. We proposed that the CO adsorption on the catalytically active site can be optimized by increasing ligand to metal back-bonding possibilities. In this case, increasing the oxidation state of Cu from 0 (Cu metal) to +1/+2 is expected to favor ligand to metal back bonding due to availability of partially filled d-orbitals at comparable energy level. Moreover, decreasing electronegativity of the anions also facilitates such ligand-to-metal backbonding by increasing electron density around the transition metal centers. Hence, it was hypothesized that Cu_2Se will show larger CO adsorption energy compared to Cu. It was also hypothesized that smaller *CO adsorption energy on specific catalyst surface will lead to preferential formation of C_1 products (CO and HCO_2H) while larger *CO adsorption energy will lead to more C2 products. However, it was also realized that very large *CO adsorption energy can potentially passivate the catalyst surface and will lead to catalyst poisoning. A series of DFT calculations were carried out for comparing the CO adsorption energy on various known catalyst surfaces along with Cu_2Se and the results are shown in Figure 8. It was observed that metals such as Ag and Au show low CO adsorption energy and they almost exclusively produce CO as has been reported previously by various research groups.[55,56] On the other hand, catalysts such as Pt, Pd and Ni showed high CO binding energy. It is well-known that these catalysts also have a high binding energy for *H and starts hydrogen evolution

reaction instead of reduction of CO_2 in aqueous medium and the catalyst is deactivated due to CO passivation by the small amounts of CO produced during continuous electroreduction of CO_2.[57] Cu metal showed a moderately larger CO adsorption energy compared to other noble metals such as Au and Ag, as shown in Figure 8. It has been reported previously that Cu is capable of producing a wide range of hydrocarbons with considerable Faradic efficiency which nicely corroborates with higher CO adsorption energy indicating longer *CO dwell time on the surface.[57] Interestingly, Cu_2Se has a moderately strong CO adsorption energy which is slightly higher than that of Cu (higher the negative value, higher the binding energy), which is favorable for further reduction of CO to carbon-rich hydrocarbon products such as ethanol and acetic acid. In addition, CO binding energy on Cu_2Se was also lower than that of the passivation level observed with other metal catalysts keeping Cu_2Se in an ideal position for CO_2 reduction. CO adsorption energy was calculated on various lattice planes of Cu_2Se and interestingly it was observed that CO adsorption energy showed minimal lattice plane dependence showing a value of -1.26 eV, for both (220) and (001) lattice planes, at ~11% surface coverage. We propose the presence of Se influences the electrocatalytic activity in multiple ways: (i) Indirect effect on electron density on catalytically active Cu center that increases CO dwell time. This has been also confirmed by the DFT studies which shows higher CO adsorption energy on Cu_2Se surface compared to bare Cu. (ii) Presence of less electronegative Se also increases electrochemical activity of Cu thereby decreasing overpotential. Such effect of enhanced electrocatalytic activity as a function of decreasing anion electronegativity has also been observed previously.[58] (iii) Presence of Se also lead to more adsorption of hydrogen in the vicinity through Lewis acid-base interaction that can lead to formation of more hydrocarbon based reduction products.

As illustrated in Figure S6, atom projected local density of states (DOS) was also calculated on surface Cu atoms before and after binding with CO for getting further insight regarding changes of electronic structure of the surface-active sites as a function of intermediate binding. It can be seen from Figure S6 that an overall stabilization of Cu 3d orbitals has taken place by moving to lower energy upon binding with CO molecules. Adsorption of CO on transition metals occur through two mechanisms contributing to the coordination bond: CO to metal σ donation through HOMO (highest occupied molecular orbitals) located on C; and metal (*d*-) to CO (π*) back donation. In Figure S6, Cu 3*d* to CO π* back donation can be identified from the contribution of CO pDOS as a low intensity peak near -3.7 eV energy range, which is comparable to previously reported results.[59] While it is imperative to do a thorough DFT study involving all the mechanistic steps of the reaction pathway and also using other possible lattice surfaces of Cu_2Se to fully understand the role of catalyst for the selective formation of specific reduction products, present DFT results indicate that Cu_2Se catalyst surface has beneficial properties for electroreduction of CO_2 to carbon-rich products by facilitating intermediate CO adsorption, which agrees with our experimental observations.

(b)

Conclusions

Copper selenide nanostructures synthesized through one-pot solvothermal synthesis were found to be highly active for electrocatalytic carbon dioxide reduction under a range of applied potential. The reduction products showed selectivity between C1 and C2 products depending on the applied potential. At high applied potential (-1.3 V) the product was identified as exclusively formic acid with a Faradaic efficiency of 94.2%. At more anodic potential (<-1.2 V) preferential formation of C2 products such as acetic acid and ethanol were observed. A maximum Faradaic efficiency for ethanol production was observed at a low applied potential of -0.6 V vs RHE. It must be noted that these are among the lowest applied potential at which C2 products have been obtained with high relative yield. The reduction products were characterized through NMR and GC-TCD spectroscopies by performing time-dependent measurements. It was also observed that H_2 was produced at high cathodic potential (>-1.2 V) indicating that Cu_2Se has reduced HER catalytic activity. This is significant since HER poses as a commendable competitor and inhibits CO2RR on the catalyst surface. Interestingly it was observed that no detectable amount of CO was formed as the reduction potential even at high negative potential. The electrocatalyst surface was further studied through DFT calculations specifically to estimate CO adsorption energy on the catalyst site, which showed moderate adsorption energy which suggests longer dwell time of the adsorbed CO on the catalyst surface leading to preferential reduction to C2 products. As mentioned above, this Cu_2Se catalyst surface can effectively reduce CO_2 to ethanol and acetic acid with high Faradaic efficiency at one of the lowest applied potential reported till date. This result along with the correlation of catalytic activity with CO adsorption energy will lead to optimal catalyst design for forming carbon-rich high-value products through CO_2 reduction.

Conflicts of interest

There are no conflicts to declare.

Acknowledgements

The authors would like to acknowledge Materials Research Center for equipment usage. JM and WPL would like to acknowledge financial support from NSF (DMR-1710313).

References

1. Gattuso, J. P.; Magnan, A.; Bille, R.; Cheung, W. W. L.; Howes, E. L.; Joos, F.; Allemand, D.; Bopp, L.; Cooley, S. R.; Eakin, C. M.; Hoegh-Guldberg, O.; Kelly, R. P.; Portner, H.-O.; Rogers, A. D.; Baxter, J. M.; Laffoley, D.; Osborn, D.; Rankovic, A.; Rochette, J.; Sumaila, U. R.; Treyer, S.;

Turley, C. Contrasting futures for ocean and society from different anthropogenic CO2 emission scenarios Science, 2015, 349, aac4722 (1-10).

2. Le Quéré, C.; Andrew, R. M.; Friedlingstein, P.; Sitch, S.; Pongratz, J.; Manning, A. C.; Korsbakken, J. I.; Peters, G. P.; Canadell, J. G.; Jackson, R. B., Global carbon budget 2017. Earth System Science Data Discussions 2017, 1-79.
3. Solomon, S.; Plattner, G.-K.; Knutti, R.; Friedlingstein, P. Irreversible climate change due to carbon dioxide emission, Proc. Natl. Acad. Sci. 2009, 106, 1704-1709.
4. Mikkelsen, M.; Jorgensen, M.; Krebs, F. C. The tetraton challenge: A review of fixation and transformation of carbon dioxide Energy Environ. Sci. 2010, 3, 43-81.
5. Bushuyev, O. S.; De Luna, P.; Dinh, C. T.; Tao, L.; Saur, G.; Lagemaat, J.; Kelley, S. O.; Sargent, E. H. What should we make with CO2 and how can we make it? Joule, 2018, 2, 825-832.
6. Zhu, D. D.; Liu, J. L.; Qiao, S. Z., Recent advances in inorganic heterogeneous electrocatalysts for reduction of carbon dioxide. Advanced materials 2016, 28 (18), 3423-3452.
7. Qiao, J.; Liu, Y.; Hong, F.; Zhang, J., A review of catalysts for the electroreduction of carbon dioxide to produce low-carbon fuels. Chemical Society Reviews 2014, 43 (2), 631-675.
8. Choi, S.; Drese, J. H.; Jones, C. W., Adsorbent Materials for Carbon Dioxide Capture from Large Anthropogenic Point Sources. ChemSusChem 2009, 2 (9), 796-854
9. Nitopi, S.; Bertheussen, E.; Scott, S. B.; Liu, X.; Engstfeld, A. K.; Horch, S.; Seger, B.; Stephens, I. E. L.; Chan, K.; Hahn, C.; Norskov, J. S.; Jaramillo, T. F.; Chorkendorf, I. Progress and perspectives of electrochemical CO2 reduction on Copper in aqueous electrolyte Chem. Rev. 2019, 119, 7610-7672.
10. Qiao, J.; Liu, Y.; Hong, F.; Zhang, J. A review of catalysts for the electroreduction of carbon dioxide to produce low-carbon fuels. Chem. Soc. Rev. 2014, 43, 631–675.
11. Li, Y.; Chan, S. H.; Sun, Q. Heterogeneous catalytic conversion of CO2: a comprehensive theoretical review, Nanoscale 2015, 7, 8663– 8683.
12. 26. Zhang, R.-Z.; Wu, B.-Y.; Li, Q.; Lu, L.-L.; Shi, W.; Cheng, P. Design strategies and mechanism studies of CO2 electroreduction catalysts based on coordination chemistry, Coord. Chem. Rev. 2020, 422, 213436 (1-28)
13. Azcarate, I.; Costentin, C.; Robert, M.; Savéant, J.-M. Through-space charge interaction substituent effects in molecular catalysis leading to the design of the most efficient catalyst of CO2-to-CO electrochemical conversion. J. Am. Chem. Soc. 2016, 138, 16639– 16644.
14. Francke, R.; Schille, B.; Roemelt, M. Homogeneously catalyzed electroreduction of carbon dioxide – Methods, mechanisms, and catalysts Chem. Rev., 2018, 118, 4631-4701.
15. Benson, E. E.; Kubiak, C. P.; Sathrum, A. J.; Smieja, J. M. Electrocatalytic and homogeneous approaches to conversion of CO2 to liquid fuels. Chem. Soc. Rev. 2009, 38, 89–99.
16. Rountree, E. S.; McCarthy, B. D.; Eisenhart, T. T.; Dempsey, J. L. Evaluation of homogeneous electrocatalysts by cyclic voltammetry Inorg. Chem. 2014, 53, 9983–10002.
17. Liu, X.; Xiao, J.; Peng, H.; Hong, X.; Chan, K.; Norskov, J. K. Understanding trends in electrochemical carbon dioxide reduction rates, Nature Commun. 2017, 8, article number 15438 (1-7)
18. Wuttig, A., Yaguchi, M., Motobayashi, K., Osawa, M. & Surendranath, Y. Inhibited proton transfer enhances Au-catalyzed CO2-to-fuels selectivity. Proc. Natl Acad. Sci. USA 2016, 113, E4585–E4593.
19. Appel, A. M. Bercaw, J. E.; Bocarsly, A, B.; Dobbek, H.; DuBois, D. L.; Dupuis, M.; Ferry, J. G.; Fujita, E.; Hille, R.; Kenis, P. J. A.; Kerfeld, C. A.; Morris, R. H.; Peden, C. H. F.; Portis, A. R.; Ragsdale, S. W.; Rauchfuss, T. B.; Reek, J. N. H. Seefeldt, L. C.; Thauer, R. K.; Waldrop, G. L. Frontiers, opportunities, and challenges in biochemical and chemical catalysis of CO2 fixation Chem. Rev. 2013, 113, 6621–6658.
20. Malik, K.; Singh, S.; Basu, S.; Verma, A. Electrochemical reduction of CO2 for synthesis of green fuel, WIREs Energy Environ 2017, 6:e244. doi: 10.1002/wene.244 (1-17).
21. Ogura K. Electrochemical reduction of carbon dioxide to ethylene: mechanistic approach. J CO2 Utilization 2013, 1, 43–49.
22. Hori, Y.; Kikuchi, K.; Suzuki, S. Production of CO and CH4 in electrochemical reduction of CO2 at metal electrodes in aqueous hydrogencarbonate solution Chem. Lett. 1985, 14, 1695–1698.
23. Yang, H.-P.; Qin, S.; Wang, H.; Lu, J.-X., Organically doped palladium: a highly efficient catalyst for electroreduction of CO 2 to methanol. Green Chemistry 2015, 17 (12), 5144-5148.
24. Chen, Y.; Li, C. W.; Kanan, M. W., Aqueous CO2 reduction at very low overpotential on oxide-derived Au nanoparticles. Journal of the American Chemical Society 2012, 134 (49), 19969-19972.
25. Jiang, K.; Kharel, P.; Peng, Y.; Gangishetty, M. K.; Lin, H.-Y. G.; Stavitski, E.; Attenkofer, K.; Wang, H., Silver Nanoparticles with Surface-Bonded Oxygen for Highly Selective CO2 Reduction. ACS Sustainable Chemistry & Engineering 2017, 5 (10), 8529-8534.
26. Hori, Y.; Kikuchi, K.; Suzuki, S. Production of CO and CH4 in electrochemical reduction of CO2 at metal electrodes in aqueous hydrogencarbonate solution Chem. Lett. 1985, 14, 1695–1698.
27. Kudo, A.; Nakagawa, S.; Tsuneto, A.; Sakata, T. Electrochemical reduction of high pressure CO2 on Ni electrodes J. Electrochem. Soc. 1993, 140, 1541–1545.
28. Reske, R.; Duca, M.; Oezaslan, M.; Schouten, K. J. P.; Koper, M. T. M.; Strasser, P. Controlling catalytic selectivities during CO2 electroreduction on thin Cu metal overlayers. J. Phys. Chem. Lett. 2013, 4, 2410–2413.
29. Rasul, S.; Anjum, D. H.; Jedidi, A.; Minenkov, Y.; Cavallo, L.; Takanabe, K. A highly selective copper–indium bimetallic electrocatalyst for the electrochemical reduction of aqueous CO2 to CO. Angew. Chem. Int. Ed. 2014, 54, 2146–2150.
30. 24. Ohya, S; Kaneco, S.; Katsumata, H.; Suzuki, T.; Ohta, K. Electrochemical reduction of CO2 in methanol with aid of CuO and Cu2O Catal. Today 2009, 148, 329–334.
31. Kuhl, K. P.; Cave, E. R.; Abram, D. N.; Jaramillo, T. F., New insights into the electrochemical reduction of carbon

dioxide on metallic copper surfaces. Energy & Environmental Science 2012, 5 (5), 7050-7059.
32. Hori, Y.; Wakebe, H.; Tsukamoto, T.; Koga, O., Electrocatalytic process of CO selectivity in electrochemical reduction of CO2 at metal electrodes in aqueous media. Electrochimica Acta 1994, 39 (11-12), 1833-1839.
33. Reske, R.; Mistry, H.; Behafarid, F.; Roldan Cuenya, B.; Strasser, P., Particle size effects in the catalytic electroreduction of CO2 on Cu nanoparticles. Journal of the American Chemical Society 2014, 136 (19), 6978-6986.
34. Tang, W.; Peterson, A. A.; Varela, A. S.; Jovanov, Z. P.; Bech, L.; Durand, W. J.; Dahl, S.; Nørskov, J. K.; Chorkendorff, I., The importance of surface morphology in controlling the selectivity of polycrystalline copper for CO2 electroreduction. Physical Chemistry Chemical Physics 2012, 14 (1), 76-81.
35. Kas, R.; Kortlever, R.; Milbrat, A.; Koper, M. T.; Mul, G.; Baltrusaitis, J., Electrochemical CO 2 reduction on Cu 2 O-derived copper nanoparticles: controlling the catalytic selectivity of hydrocarbons. Physical Chemistry Chemical Physics 2014, 16 (24), 12194-12201.
36. Whipple, D. T.; Kenis, P. J., Prospects of CO2 utilization via direct heterogeneous electrochemical reduction. The Journal of Physical Chemistry Letters 2010, 1 (24), 3451-3458.
37. Maurin, A.; Robert, M., Noncovalent immobilization of a molecular iron-based electrocatalyst on carbon electrodes for selective, efficient CO2-to-CO conversion in water. Journal of the American Chemical Society 2016, 138 (8), 2492-2495.
38. Xu, J.; Natsui, K.; Naoi, S.; Nakata, K.; Einaga, Y., Effect of doping level on the electrochemical reduction of CO2 on boron-doped diamond electrodes. Diamond and Related Materials 2018, 86, 167-172.
39. Neaţu, S. t.; Maciá-Agulló, J. A.; Concepción, P.; Garcia, H., Gold–copper nanoalloys supported on TiO2 as photocatalysts for CO2 reduction by water. Journal of the American Chemical Society 2014, 136 (45), 15969-15976.
40. Albo, J.; Sáez, A.; Solla-Gullón, J.; Montiel, V.; Irabien, A., Production of methanol from CO2 electroreduction at Cu2O and Cu2O/ZnO-based electrodes in aqueous solution. Applied Catalysis B: Environmental 2015, 176, 709-717.
41. Asadi, M.; Kim, K.; Liu, C.; Addepalli, A. V.; Abbasi, P.; Yasaei, P.; Phillips, P.; Behranginia, A.; Cerrato, J. M.; Haasch, R., Nanostructured transition metal dichalcogenide electrocatalysts for CO2 reduction in ionic liquid. Science 2016, 353 (6298), 467-470.
42. Ahn, S. T.; Abu-Baker, I.; Palmore, G. T. R., Electroreduction of CO2 on polycrystalline copper: Effect of temperature on product selectivity. Catalysis Today 2017, 288, 24-29.
43. Hori, Y.; Takahashi, I.; Koga, O.; Hoshi, N., Selective formation of C2 compounds from electrochemical reduction of CO2 at a series of copper single crystal electrodes. The Journal of Physical Chemistry B 2002, 106 (1), 15-17.
44. Chen, Y.; Kanan, M. W., Tin oxide dependence of the CO2 reduction efficiency on tin electrodes and enhanced activity for tin/tin oxide thin-film catalysts. Journal of the American Chemical Society 2012, 134 (4), 1986-1989.
45. Jitaru, M.; Lowy, D.; Toma, M.; Toma, B.; Oniciu, L., Electrochemical reduction of carbon dioxide on flat metallic cathodes. Journal of Applied Electrochemistry 1997, 27 (8), 875-889.
46. Albo, J.; Sáez, A.; Solla-Gullón, J.; Montiel, V.; Irabien, A., Production of methanol from CO2 electroreduction at Cu2O and Cu2O/ZnO-based electrodes in aqueous solution. Applied Catalysis B: Environmental 2015, 176, 709-717.
47. R. García-Muelas, F. Dattila, T. Shinagawa, A. J. Martín, J. Pérez-Ramírez and N. López, Origin of the Selective Electroreduction of Carbon Dioxide to Formate by Chalcogen Modified Copper, J. Phys. Chem. Lett., 2018, 9, 24, 7153–7159.
48. Shinagaya, T.; Larrazabai, G. O.; Martin, A. J.; Krumeich, F.; Perez-Ramirez, J. *ACS Catalysis* **2018**, *8*, 827-844.
49. J. Masud, W. P. R. Liyanage, X. Cao, A. Saxena and M. Nath, Copper Selenides as High-Efficiency Electrocatalysts for Oxygen Evolution Reaction, *ACS Appl. Energy Mater. 2018, 1, 8, 4075–4083*.
50. Zhu, Q., Sun, X., Yang, D. et al. Carbon dioxide electroreduction to C2 products over copper-cuprous oxide derived from electrosynthesized copper complex. Nat Commun 10, 3851 (2019)
51. Z. Chen, K. Mou, S. Yao and L. Liu, Highly selective electrochemical reduction of CO2 to formate on metal-free nitrogen-doped PC61BM, J. Mater. Chem. A, J. Mater. Chem. A, 2018,6, 11236-11243, DOI:10.1039/c8ta03328e..
52. Sun, Z., Ma, T., Tao, H., Fan, Q., & Han, B. (2017). Fundamentals and challenges of electrochemical CO2 reduction using two-dimensional materials. Chem, 3(4), 560-587.
53. Hansen, H. A., Varley, J. B., Peterson, A. A., & Nørskov, J. K. (2013). Understanding trends in the electrocatalytic activity of metals and enzymes for CO2 reduction to CO. The journal of physical chemistry letters, 4(3), 388-392.
54. Yang, D., Zhu, Q., Chen, C., Liu, H., Liu, Z., Zhao, Z. & Han, B. (2019). Selective electroreduction of carbon dioxide to methanol on copper selenide nanocatalysts. Nature communications, 10(1), 1-9.
55. Rosen, J., Hutchings, G. S., Lu, Q., Rivera, S., Zhou, Y., Vlachos, D. G., & Jiao, F. (2015). Mechanistic insights into the electrochemical reduction of CO2 to CO on nanostructured Ag surfaces. Acs Catalysis, 5(7), 4293-4299.
56. Back, S., Yeom, M. S., & Jung, Y. (2015). Active sites of Au and Ag nanoparticle catalysts for CO2 electroreduction to CO. ACS Catalysis, 5(9), 5089-5096.
57. U. De Silva, J. Masud, N. Zhang, Y. Hong, W. P. R. Liyanage, M. Asle Zaeem and M. Nath, Nickel telluride as a bifunctional electrocatalyst for efficient water splitting in alkaline medium, *J. Mater. Chem. A*, 2018,**6**, 7608-7622
58. Chatterjee, S., Griego, C., Hart, J. L., Li, Y., Taheri, M. L., Keith, J., & Snyder, J. D. (2019). Free standing nanoporous palladium alloys as CO poisoning tolerant electrocatalysts

for the electrochemical reduction of CO2 to formate. ACS Catalysis, 9(6), 5290-5301.

59. Soon, A., Söhnel, T., & Idriss, H. (2005). Plane-wave pseudopotential density functional theory periodic slab calculations of CO adsorption on Cu2O (1 1 1) surface. Surface science, 579(2-3), 131-140.